

Mass attenuation coefficients, effective atomic numbers and electron densities of some contrast agents for computed tomography

Mohammed Sultan Al-Buriahi*, Baris T. Tonguc

Department of Physics, Sakarya University, Sakarya, Turkey



ARTICLE INFO

Keywords:

Mass attenuation coefficient
Effective atomic number
Electron density
CT contrast agent
Geant4

ABSTRACT

In the clinical computed tomography (CT) examinations, a photon is attenuated as it passes a patient by tissues and contrast agents (CAs). The CAs can increase the visibility of internal structures or fluids within the patient. In this work, we have investigated the photon interaction parameters of some CT contrast agents such as iotrolan, iodixanol, iohexol, ioxilan, ioversol, and iomeprol. The mass attenuation coefficients (μ/ρ) of these contrast agents have been determined using Geant4 code in the energy range from 1 keV to 1 MeV for total photon interaction. The validity of the Geant4 code was verified by comparing the simulation results with those calculated by the XCOM program. A very good agreement was observed between μ/ρ values obtained by both Geant4 and XCOM codes. The μ/ρ values were then used to estimate the effective atomic numbers (Z_{eff}) and electron densities (N_{eff}) for the selected CT contrast agents. It was found that the values of μ/ρ , Z_{eff} and N_{eff} depend on the photon energy and increase with increasing iodine concentration in the composition of CAs. Also, the Z_{eff} values were observed in the range of 6–50 and the N_{eff} values were observed in the range of 2–21 (10^{23} electron/g). The present study would be helpful to develop new CT contrast agents to serve in vivo imaging applications.

1. Introduction

A contrast agent contains at least one heavy element with high K-edge energy (e.g., barium or iodine) that provides greater absorption and scattering of photons in a target tissue. Therefore, the radiologist has to choose a certain contrast agent knowing its attenuation features and balancing them with the clinical interests for an accurate diagnosis. Over the past 10 years, there is a tremendous attention among researchers to investigate the properties of the CAs in order to increment the quality of CT scans as well as to provide the maximum safety for the patient (Bae, 2010; Caschera et al., 2016; Lusic and Grinstaff, 2012; Berger et al., 2017). The contrast agents can be categorised according to their structure as; monomer and dimer (Lee et al., 2013; Caschera et al., 2016). Also, they can be classified according to their charge as; ionic and nonionic (Bae, 2010). The ionic contrast agents have toxicity more than nonionic contrast agents that currently use in CT scan (Thomsen et al., 2014).

One way to study the photon interaction with matter is Monte Carlo (MC) simulation method. The MC method is a widespread technique to simulate the track structures and the electromagnetic processes in specific material, especially by using Geant4 (Agostinelli et al., 2003), MCNPX (Sayed et al., 2019a) and FLUKA (Sharma et al., 2019)

programs. By MC method, one can predict the experimental results especially when the experiments are rarely implemented. Furthermore, the simulation model provides flexibility to apply the wanted scenario in software environment without the difficulties of the experiment. The literature was enriched by several successful publications based on different Geant4 codes (Al-Buriahi and Rammah, 2019). Francis et al., studied electrons, protons and alpha particles as they pass through water by using Geant4 simulations (Francis et al., 2011). Shimizu et al., compared the experimental cross section values of water for protons with the results of Geant4 (Shimizu et al., 2009). Bordage et al., investigated the novel models for electrons in water by Geant4 simulations (Bordage et al., 2016). Singh has considerable studies for determination of attenuation coefficients by Geant4 toolkit for thermoluminescent agents, nuclear track detectors and some polymers (Singh et al., 2014, 2015a, 2015b, 2015c).

The studies of photon interaction with matter in terms of mass attenuation coefficient (μ/ρ), effective atomic number (Z_{eff}), and electron density (N_{eff}), led to develop many materials for various applications (Erik et al., 2019; Kilicoglu et al., 2019; Tekin et al., 2019). In medical field, the knowledge about how the photons beam interacts with tissues and tissue equivalents leads to progress the clinical diagnosis by the CT scan (Kurudirek, 2014a, 2014b; Singh and Badiger, 2013). Also, gamma

* Corresponding author.

E-mail addresses: mburiahi@gstd.sci.cu.edu.eg, mohammed.al-buriahi@ogr.sakarya.edu.tr (M.S. Al-Buriahi).

shielding materials (concrete, glass, alloy. ans .etc) were investigated in the terms of photon interaction parameters elsewhere (Sayyed et al., 2017; Issa et al., 2018; Kurudirek et al., 2018; Gaikwad et al., 2018). However, although the contrast agents are integral part of medical imaging and dose calculation (Choi et al., 2006; Ramm et al., 2001), such studies for the CT contrast agents are completely missing in literature. Consequently, A full understanding of the photon interaction with these contrast agents has is to be achieved.

In the present work, the CT contrast agents have been studied for the first time in terms of the attenuation parameters (μ/ρ , Z_{eff} , N_{eff}). For this purpose the Geant4 simulations were carried out to determine the mass attenuation coefficients for the samples at energies from 1 keV to 1 MeV. The simulated values were compared to the theoretical results of XCOM program. The μ/ρ values were used to calculate the effective atomic numbers and the electron densities for the CT contrast agents involved. To mimic the real scans, the effective atomic numbers relative to water were also calculated. Moreover, the effect of iodine concentration on the attenuation parameters and the behaviour of the attenuation parameters at the absorption edges of iodine were also discussed.

2. Materials and methods

Names, chemical compositions and weight fractions of elements for the selected CT contrast agents are listed in Table 1. The more knowledge about these contrast agents can be found elsewhere (Caschera et al., 2016; Lee et al., 2013; Thomsen et al., 2014).

2.1. Geant4 simulation code

The geometry of Monte Carlo simulation has been arrangement by using Geant4 as mentioned in (Tonguc et al., 2018; Aşkın et al., 2019; Sayyed et al., 2019b). The photons have been gunned from monoenergetic source to hit a slab of the samples. Then, the transmitted photons have been recorded by using sodium iodide (NaI) detector. Lead (Pb) has been used to collimate gamma source and to shield the used detector. The energy source has been defined in the range of 1 keV-1 MeV. Also, the CT contrast agents have been modeled with respect to their atomic number, mass number and weight fractions of the elements. The energy cut-off has been set to 2.93 keV and 10^6 photons have been shot for each sample at every energy separately. Geant4 simulations have carried out to determine the μ/ρ for the CT contrast agents involved by using the transmission method based on Beer–Lambert law ($I_t = I_0 e^{-\mu_m x}$), where I_0 is the incident intensity and I_t is the transmitted intensity, μ_m is the mass attenuation coefficient and x is the thickness of the absorber in unit of g/cm². XCOM program was also used to compute the μ_m for the samples involved. This program is based on the mixture rule ($\mu_m = \sum_i w_i (\mu_m)_i$) (Al-Buriah et al., 2019). This method is widely used in literature to calculate the attenuation coefficients for different materials (Tonguc et al., 2018).

2.2. Effective atomic number (Z_{eff}) and electron density (N_{eff})

Z_{eff} of the photon interaction can be obtained by using the mass

Table 1

Name, chemical formula and weight fractions of elements for the selected CT contrast agents.

Name	Formula	H	C	N	O	I
Iotrolan	$C_{37}H_{48}I_6N_6O_{18}$	0.02975	0.27327	0.05168	0.17709	0.46821
Iodixanol	$C_{35}H_{44}I_6N_6O_{15}$	0.02861	0.27118	0.05421	0.15482	0.49118
Iohexol	$C_{19}H_{26}I_3N_3O_9$	0.03191	0.27792	0.05117	0.17536	0.46364
Ioxilan	$C_{18}H_{24}I_3N_3O_8$	0.03058	0.27328	0.05312	0.16179	0.48123
Ioversol	$C_{18}H_{24}I_3N_3O_9$	0.02997	0.26786	0.05206	0.17841	0.47170
Iomeprol	$C_{17}H_{22}I_3N_3O_8$	0.02854	0.26276	0.05407	0.16471	0.48992

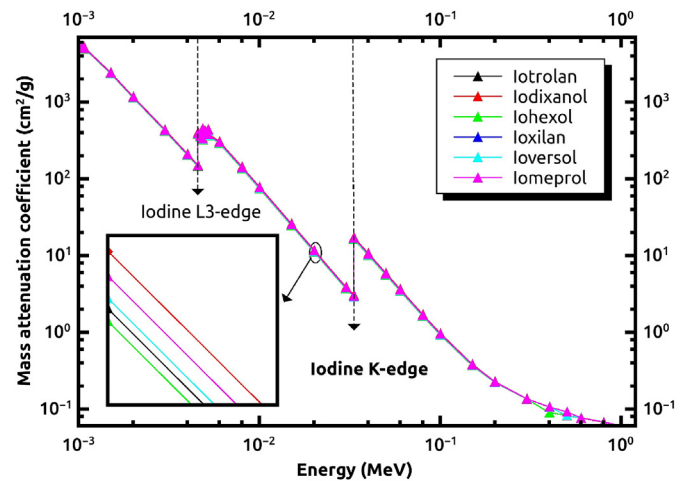


Fig. 1. Mass attenuation coefficients as a function of photon energy for the CT contrast agents by Geant4 simulations.

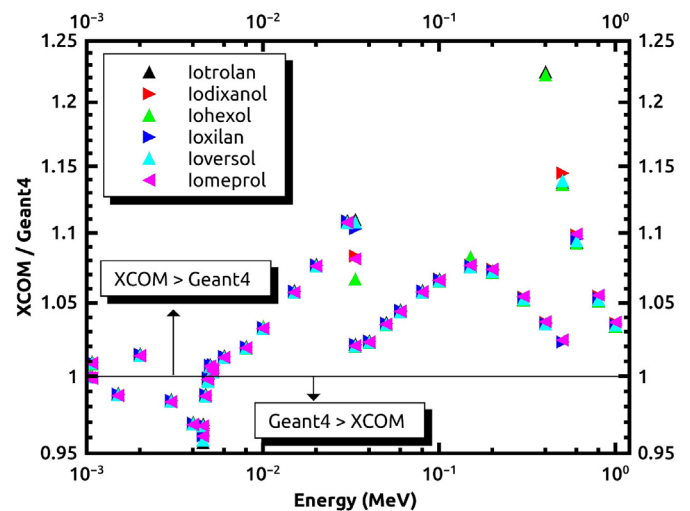


Fig. 2. Comparison between the mass attenuation coefficients determined from Geant4 simulations and those obtained from XCOM program for the CT contrast agents.

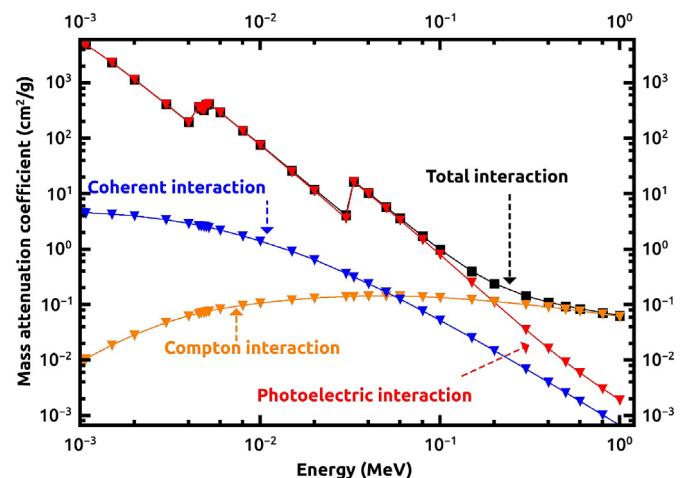


Fig. 3. Typical example of the partial attenuation processes in the case of iodixanol in the energy range between 1 keV and 1 MeV using Geant4 package.

Table 2

Effective atomic number (Z_{eff}) and Effective electron density ($N_{eff} \times 10^{23}$ electron/g) values for total photon interaction for iomeprol, ioversol and ioxilan.

E (MeV)	Iomeprol		Ioversol		Ioxilan	
	Z_{eff}	N_{eff}	Z_{eff}	N_{eff}	Z_{eff}	N_{eff}
1.00E-03	19.830	8.144	19.143	8.141	19.572	8.343
1.04E-03	20.162	8.281	19.463	8.277	19.901	8.483
1.07E-03	20.202	8.297	19.501	8.294	19.942	8.501
1.07E-03	20.599	8.460	19.885	8.457	20.334	8.668
1.50E-03	22.552	9.262	21.773	9.260	22.277	9.496
2.00E-03	24.092	9.895	23.271	9.897	23.811	10.150
3.00E-03	26.234	10.775	25.367	10.788	25.949	11.062
4.00E-03	27.763	11.403	26.873	11.429	27.476	11.712
4.56E-03	28.476	11.696	27.578	11.728	28.188	12.016
4.56E-03	40.039	16.445	39.288	16.709	39.807	16.969
4.70E-03	40.339	16.568	39.598	16.841	40.111	17.098
4.85E-03	40.555	16.657	39.822	16.936	40.330	17.192
4.85E-03	43.072	17.691	42.440	18.049	42.879	18.278
5.00E-03	43.322	17.793	42.701	18.160	43.132	18.386
5.19E-03	44.484	18.271	43.919	18.678	44.312	18.889
5.19E-03	43.453	17.847	42.837	18.218	43.265	18.443
6.00E-03	45.004	18.484	44.464	18.910	44.839	19.114
8.00E-03	45.692	18.767	45.188	19.218	45.533	19.410
1.00E-02	46.025	18.903	45.539	19.367	45.862	19.550
1.50E-02	45.769	18.798	45.270	19.253	45.560	19.421
2.00E-02	44.379	18.227	43.809	18.631	44.084	18.792
3.00E-02	39.303	16.143	38.527	16.385	38.791	16.536
3.32E-02	37.345	15.338	36.511	15.528	36.772	15.675
3.32E-02	49.101	20.167	48.813	20.760	48.907	20.848
4.00E-02	47.525	19.519	47.136	20.046	47.249	20.141
5.00E-02	44.635	18.332	44.085	18.749	44.227	18.853
6.00E-02	41.245	16.940	40.541	17.242	40.712	17.354
8.00E-02	34.075	13.995	33.171	14.107	33.371	14.225
1.00E-01	27.663	11.362	26.721	11.364	26.915	11.473
1.50E-01	17.447	7.166	16.707	7.105	16.830	7.174
2.00E-01	12.799	5.257	12.256	5.212	12.323	5.253
3.00E-01	9.388	3.856	9.029	3.840	9.047	3.856
4.00E-01	8.277	3.399	7.985	3.396	7.985	3.404
5.00E-01	7.795	3.201	7.533	3.204	7.525	3.208
6.00E-01	7.548	3.100	7.302	3.105	7.290	3.107
8.00E-01	7.308	3.002	7.078	3.010	7.062	3.010
1.00E+00	7.199	2.957	6.976	2.967	6.958	2.966

attenuation coefficient of the contrast agents ($(\mu_m)_{CA}$). The $(\mu_m)_{CA}$ values have been used to calculate the total molecular cross section (σ_m) by using the equation (Kurudirek, 2017),

$$\sigma_m = \frac{M}{N_A} (\mu_m)_{CA} \quad (1)$$

where $M = \sum_i n_i A_i$ is the molecular weight of the contrast agents, N_A is the Avogadro's number, n_i and A_i is the total number of atoms and the atomic weight of i^{th} element in the contrast agent. The effective atomic cross section (σ_a) has been also determined by the following relation (Sayed et al., 2019c),

$$\sigma_a = \frac{(\mu_m)_{CA}}{N_A \sum_i w_i/A_i} = \frac{1}{N_A} \sum_i f_i A_i (\mu_m)_i = \frac{\sigma_m}{\sum_i n_i} \quad (2)$$

where f_i is the fractional abundance of the each constituent element for the contrast agents, providing that $\sum_i f_i = 1$. Similarly, effective electronic cross section (σ_e) is given by the equation (Turhan et al., 2019),

$$\sigma_e = \frac{1}{N_A} \sum_i \frac{f_i A_i}{Z_i} (\mu_m)_i = \frac{\sigma_m}{Z_{eff}} \quad (3)$$

where Z_i is the atomic number of i^{th} element in the contrast agent. Thereafter, one can obtain the effective atomic number Z_{eff} as (Sayed et al., 2019c),

$$Z_{eff} = \frac{\sigma_a}{\sigma_e} \quad (4)$$

The effective electron densities are also calculated from the values

Table 3

Effective atomic number and Effective electron density ($N_{eff} \times 10^{23}$ electron/g) values for total photon interaction for iohexol, iodixanol and iotrolan.

E (MeV)	Iohexol		Iodixanol		Iotrolan	
	Z_{eff}	N_{eff}	Z_{eff}	N_{eff}	Z_{eff}	N_{eff}
1.00E-03	18.910	8.321	19.932	8.208	19.027	8.102
1.04E-03	19.227	8.460	20.268	8.346	19.345	8.238
1.07E-03	19.266	8.477	20.309	8.363	19.384	8.255
1.07E-03	19.645	8.644	20.708	8.527	19.765	8.417
1.50E-03	21.523	9.471	22.684	9.341	21.648	9.219
2.00E-03	23.014	10.127	24.241	9.982	23.143	9.855
3.00E-03	25.104	11.046	26.403	10.872	25.237	10.747
4.00E-03	26.604	11.706	27.942	11.506	26.742	11.388
4.56E-03	27.305	12.015	28.659	11.801	27.447	11.688
4.56E-03	39.061	17.188	40.193	16.551	39.180	16.685
4.70E-03	39.373	17.325	40.491	16.673	39.491	16.817
4.85E-03	39.599	17.424	40.706	16.762	39.716	16.913
4.85E-03	42.247	18.590	43.202	17.790	42.348	18.034
5.00E-03	42.511	18.706	43.450	17.892	42.611	18.146
5.19E-03	43.745	19.249	44.601	18.366	43.837	18.668
5.19E-03	42.648	18.766	43.580	17.945	42.749	18.204
6.00E-03	44.294	19.490	45.116	18.578	44.387	18.902
8.00E-03	45.012	19.806	45.795	18.858	45.117	19.213
1.00E-02	45.343	19.952	46.121	18.992	45.471	19.364
1.50E-02	44.961	19.784	45.849	18.879	45.203	19.250
2.00E-02	43.316	19.060	44.444	18.301	43.735	18.625
3.00E-02	37.595	16.543	39.341	16.200	38.433	16.366
3.32E-02	35.460	15.603	37.375	15.390	36.411	15.506
3.32E-02	48.443	21.316	49.113	20.224	48.778	20.772
4.00E-02	46.603	20.506	47.533	19.573	47.089	20.053
5.00E-02	43.296	19.051	44.640	18.382	44.019	18.745
6.00E-02	39.516	17.388	41.247	16.985	40.459	17.229
8.00E-02	31.844	14.012	34.071	14.030	33.068	14.082
1.00E-01	25.333	11.147	27.655	11.388	26.618	11.335
1.50E-01	15.579	6.855	17.433	7.178	16.634	7.084
2.00E-01	11.374	5.005	12.783	5.264	12.208	5.199
3.00E-01	8.376	3.685	9.370	3.858	9.004	3.834
4.00E-01	7.414	3.262	8.258	3.401	7.968	3.393
5.00E-01	6.999	3.080	7.776	3.202	7.520	3.202
6.00E-01	6.787	2.986	7.529	3.100	7.291	3.105
8.00E-01	6.582	2.896	7.290	3.002	7.069	3.010
1.00E+00	6.488	2.855	7.180	2.957	6.967	2.967

of Z_{eff} as (Tekin et al., 2019):

$$N_{eff} = N_A \frac{nZ_{eff}}{\sum_i n_i A_i} \quad (\text{electrons/g}) \quad (5)$$

Another useful parameter is the effective atomic number relative to water (ZRW_{eff}) that usually used to mimic the scan in human body. ZRW_{eff} values have been obtained by the ratio (Tekin et al., 2019):

$$ZRW_{eff} = \frac{(Z_{eff})_{CA}}{(Z_{eff})_{water}} \quad (6)$$

A single-valued effective atomic numbers (ZX_{eff}) were directly calculated by using XMuDat software based on the equation (Nowotny, 1998):

$$ZX_{eff} = \sum_i (\alpha_i Z_i^{m-1})^{1/(m-1)} \quad (7)$$

where α_i is the fractional number of the electrons of the i^{th} element and m is a constant between 3 and 5. Also, from the chemical formula of the CT contrast agents, one can calculate the mean atomic number, $\langle Z \rangle$ such as $\langle Z \rangle = \sum_i n_i Z_i / n$.

3. Results and discussion

Fig. 1 shows the mass attenuation coefficients obtained from Geant4 simulations for the CT contrast agents in the energy region between 1 keV and 1 MeV. It is clear that the behaviour of the mass attenuation coefficients strongly depends on the photon energy and the chemical

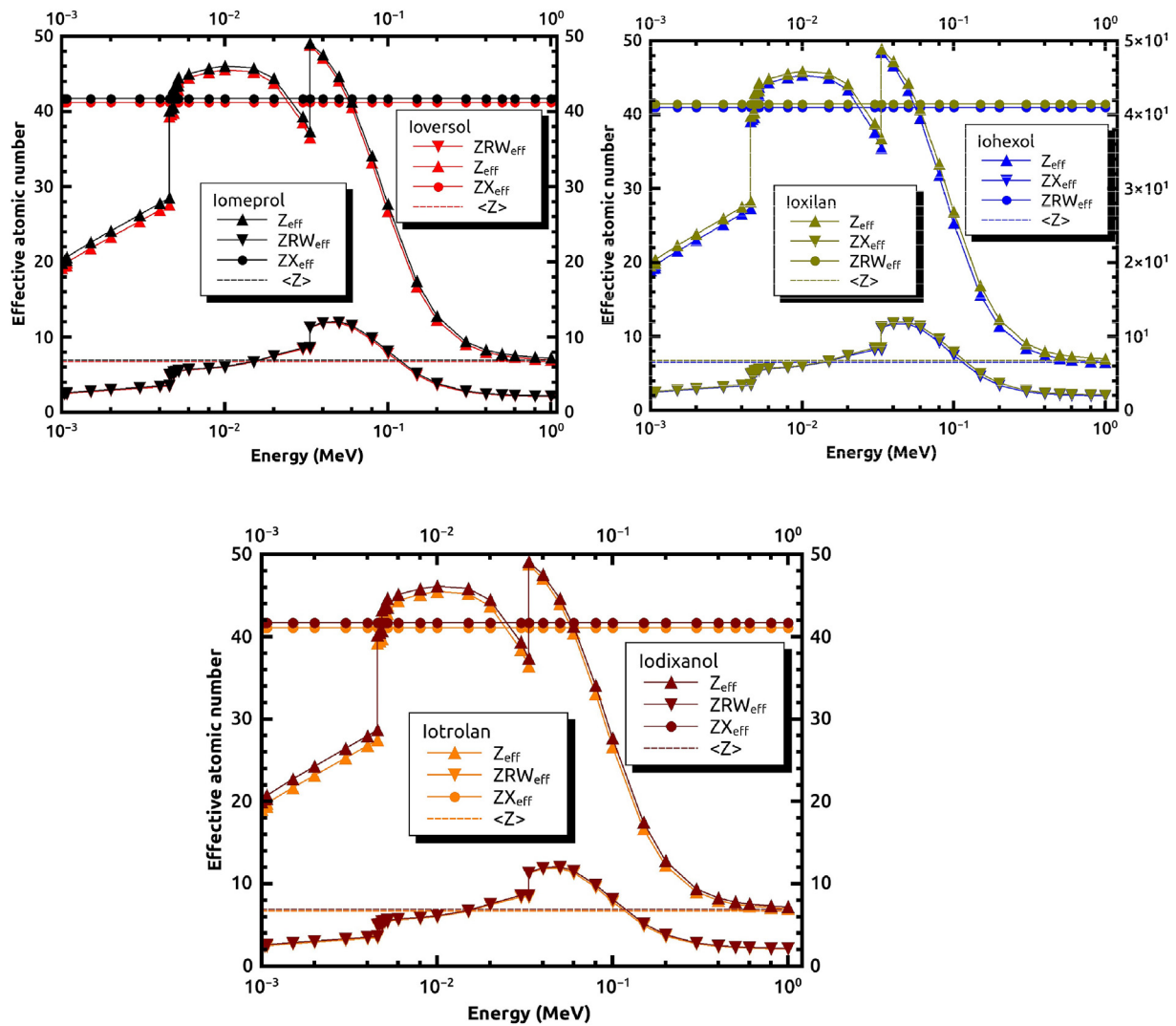


Fig. 4. Effective atomic number (Z_{eff}), effective atomic number relative to water (ZRW_{eff}), single-valued effective atomic number (ZX_{eff}) and mean atomic number ($\langle Z \rangle$) for the total photon interaction of the CT contrast agents.

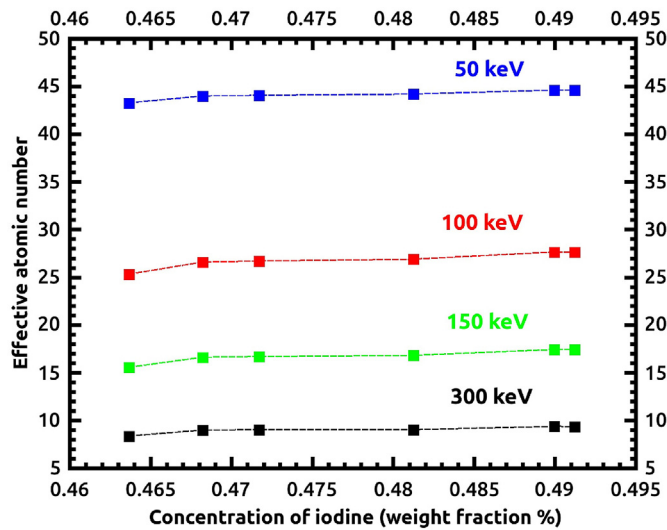


Fig. 5. Effective atomic number (Z_{eff}) of the CT contrast agents with different concentration of iodine at different photon energies.

composition of the CT contrast agents studied. The μ/ρ values of a given CT contrast agents rapidly minify with increasing the photon energy due to the partial photon interactions (e.g. photoelectric effect, Compton scattering, .ect.). On the other hand, the chemical composition dependence can be noticed by glancing to the zooming part in Fig. 1. For example, the ascending order of the weight fraction of iodine in the molecule is as: iohexol (0.464%), iotrolan (0.468%), ioversol (0.472%), ioxilan (0.481%), iomeprol (0.490%), iodixanol (0.491%). Then, One can distinguish the chemical composition dependence of mass attenuation coefficients for the CT contrast agents at a given energy. Such that the iodixanol (the red line in Fig. 1) with the highest concentration of iodine (0.491%) has the highest values of the mass attenuation coefficients.

The Geant4 simulation data of the mass attenuation coefficients has been compared with the theoretical values of XCOM program in Fig. 2. It is clear that there is a satisfactory agreement between the simulation results and the theoretical values at the commonly used diagnostic energies < 400 keV, while the maximum discrepancies of 23 % have been observed at 400 keV. Furthermore, almost the all XCOM values come bigger than the simulation results. These discrepancies reflect the effect of the chemical composition of the CT contrast agents and the mixture rule method (Medhat and Singh, 2014). By the looking to these discrepancies between the simulation results and theoretical values, it is

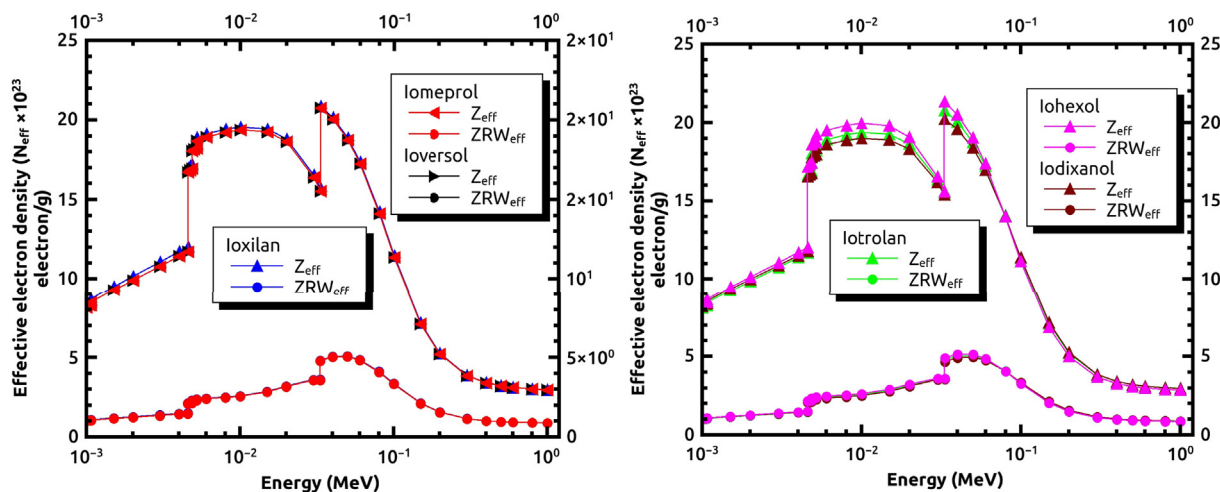


Fig. 6. Effective electron density (N_{eff}) and effective electron density relative to water (NRW_{eff}) for the total photon interaction of the CT contrast agents.

recommended to use the simulation values. The reason is that although the uncertainty of the theoretical XCOM values is (5%) (Hubbell, 1979, 1999; Hubbell et al., 1975), the Geant4 simulation has uncertainties about (3%) and also has several respective strengths if comparing to NIST-XCOM database (Amako et al., 2005).

The μ/ρ results from the partial photon interactions as shown in Fig. 3 in the case of iodixanol. It is clearly seen that the total attenuation (or μ/ρ) is largely, but not exclusively, dependent on the photoelectric interaction. In fact, this attenuation results from three categories of photon interaction according to entire energy region considered. The coherent interaction is most likely to occur in very low energies but its contribution is minor and neglected if comparing with the contribution of the photoelectric interaction. As photon energy increases the probability of Compton interaction grows up and this interaction dominates the attenuation process at intermediate photon energies ($E > 0.2$ MeV). It is worth mentioning that the photoelectric is more preferable in medical applications due to the photoelectric interaction depends on the atomic number of the absorbing object and the Compton interaction depends on the electron density. Also, the Compton interaction is undesirable effect in medical images as well as in radiotherapy because of that the ejected photon may scatter in all directions and this causes the decrease in the contrast of images and increase in radiation dose to patients. The photoelectric interaction is the dominating mechanism in low photon energies where the binding energies (absorption edges) of most elements take place. Thus, when the photoelectric interaction occurs at those energies the sharp peaks appear reflecting the existence of two values of the attenuation parameter at the same energy. These peaks become more obvious at the binding energy for the relatively high atomic number elements (e.g. iodine).

The present of iodine in the studied CT contrast agents influences all the attenuation properties (μ/ρ , Z_{eff} , and N_{eff}), such that two values of μ/ρ , Z_{eff} , and N_{eff} have been observed at the absorption edges of iodine as shown in Figs. 1, 4 and 6. Also, Tables 2 and 3 are included the values of iodine absorption edges that are (M1 = 1.07 keV), (L3 = 4.56 keV), (L2 = 4.85 keV), (L1 = 5.19 keV) and (K = 33.17 keV).

It can be noticed that there are significant jumps at absorption edges of L3 and K due to that the probability of the photoelectric effect becomes high for the inner electrons which are very close to nucleus. The effective atomic number Z_{eff} that have been calculated from chemical composition and μ/ρ of the CT contrast agents, is shown in Fig. 4. The variation of Z_{eff} with energy confirm the idea of Hine who noticed that the atomic number of the multi-element agents is not constant but varies with energy (Hine, 1952). The energy dependence of Z_{eff} can be explained by the partial photon processes. The Z_{eff} values increase in the

region of low energies (1 keV–40 keV) with a sudden jumps at the absorption edge of iodine due to the major contribution of photoelectric effect in this region.

The maximum value of Z_{eff} occurs at iodine K-edge (33.2 keV) for all the CT contrast agents studied. After that, the dominance of Compton scattering leads to diminish the Z_{eff} values. In Fig. 4, the effective atomic numbers of the CT contrast agents have been compared with ZRW_{eff} , $\langle Z \rangle$, and ZX_{eff} . The ZRW_{eff} values have a weak variation versus the photon energies, such that they do not pass up to 12. The $\langle Z \rangle$ are in good agreements with lower Z_{eff} values while the ZX_{eff} approach to the higher values of Z_{eff} . For example in the case of iomeprol, The $ZX_{eff} = 41.72 \approx Z_{eff}$ at the photon energies of 60 keV and 48 keV, while $\langle Z \rangle = 6.9 \approx Z_{eff}$ at the photon energies ≥ 800 keV.

The effective atomic numbers have been plotted with respect to the concentration of iodine in the CT contrast agents at different photon energies as shown in Fig. 5. It can be easily seen that there is an increase in Z_{eff} values as the concentration of iodine increases. This is because of the mole fraction of the high Z element (iodine) increased at the expense of the other low Z elements. Moreover, it is clearly that the effective atomic numbers decrease as the photon energy raises and this is due to the high energy photons can penetrate deeply in the absorber material (say a contrast agent) without making any interaction. As a result of this, the maximum value of Z_{eff} occurs at 33.2 keV in iodixanol who has the highest concentration (0.491%) of iodine. The results of N_{eff} and NRW_{eff} are shown in Fig. 6. It can be seen that the effective electron densities vary from a higher value at lower energies to a lower value at higher energies with a peak due to photoelectric effect near the K-absorption edge of iodine element in the contrast agent. In contrast, the effective electron densities relative to water for all selected contrast agents do not show strong energy dependence such that it takes values between 0 and 4 along considered energy range. This behaviour of the effective electron densities can be explained in a similar manner of the effective atomic numbers due to the linear relation between N_{eff} and Z_{eff} .

3. Conclusion

In this work, the photon interaction parameters of CT contrast agents have been studied in the energy range between 1 keV and 1 MeV. The values of the mass attenuation coefficients have been extracted from Geant4 simulations and compared with those calculated by the XCOM program. A good agreement was observed between the results of Geant4 and XCOM. The values of Z_{eff} and N_{eff} have been calculated and compared with those of relative to water, single-valued, and mean atomic numbers for each CT contrast agent. It was noted that both of

Z_{eff} and N_{eff} have higher values at lower energies and lower values at higher energies. The low values of Z_{eff} are close to the mean atomic numbers, while the high values of Z_{eff} are close to single-valued of the effective atomic numbers for the present CT contrast agents. Moreover, it was found that the photon interaction parameters of the CT contrast agents tend to increase with increasing iodine concentration. Furthermore, the absorption edges of iodine influence the photon interaction parameters, such that μ/ρ , Z_{eff} , and N_{eff} possess two values at those energies. It can be concluded that for CT scans applications the selection of an appropriate contrast agent can be done based on data of Z_{eff} , N_{eff} , consideration of iodine concentration and also, according to the desired examination. The results were listed in tables because of their potential importance

Acknowledgement

The corresponding author would like to thanks Prof. Murat Kurudirek, department of Physics, Ataturk University, Turkey for his useful discussion.

References

- Agostinelli, S., Allison, J., Amako, K., Apostolakis, J., Araujo, H., Arce, P., et al., 2003. GEANT4 - a simulation toolkit. *Nucl. Instrum. Methods Phys. Res. Sect. A* **506** (3), 250–303. [https://doi.org/10.1016/S0168-9002\(03\)01368-8](https://doi.org/10.1016/S0168-9002(03)01368-8). arXiv: 1005.0727v1.
- Al-Buriah, M., Rammah, Y., 2019. Electronic polarizability, dielectric, and gamma-ray shielding properties of some tellurite-based glasses. *Appl. Phys. A* **125** (10), 678.
- Al-Buriah, M.S., Arslan, H., Tonguc, B.T., 2019. Investigation of photon energy absorption properties for some biomolecules. *Nucl. Sci. Tech.* **30** (7), 103.
- Amako, K., Guatelli, S., Ivanchenko, V.N., Maire, M., Mascialino, B., Murakami, K., et al., 2005. Comparison of Geant4 electromagnetic physics models against the NIST reference data. *IEEE Trans. Nucl. Sci.* **52** (4), 910–918. <https://doi.org/10.1109/TNS.2005.852691>.
- Aşkın, A., Sayyed, M., Sharma, A., Dal, M., El-Mallawany, R., Kaçal, M., 2019. Investigation of the gamma ray shielding parameters of (100-x)[0.5 li₂o–0.1 b₂o₃–0.4 p₂o₅]–xteo₂ glasses using geant4 and fluka codes. *J. Non-Cryst. Solids* **521**, 119489.
- Bae, K.T., 2010. Intravenous contrast medium administration and scan timing at ct: considerations and approaches. *Radiology* **256** (1), 32–61.
- Berger, M., Bausier, M., Frenzel, T., Hilger, C.S., Jost, G., Lauria, S., et al., 2017. Hafnium-based contrast agents for X-ray computed tomography. *Inorg. Chem.* **56** (10), 5757–5761. <https://doi.org/10.1021/acs.inorgchem.7b00359>.
- Bordage, M.C., Bordes, J., Edel, S., Terrissol, M., Franceries, X., Bardiès, M., et al., 2016. Physica Medica Implementation of new physics models for low energy electrons in liquid water in Geant4-DNA. *Phys. Med.* **32** (12), 1833–1840. <https://doi.org/10.1016/j.ejmp.2016.10.006>. URL: <https://doi.org/10.1016/j.ejmp.2016.10.006>.
- Caschera, L., Lazzara, A., Piergallini, L., Ricci, D., Tuscano, B., Vanzulli, A., 2016. Contrast agents in diagnostic imaging: present and future. *Pharmacol. Res.* **110**, 65–75. <https://doi.org/10.1016/j.phrs.2016.04.023>. URL: <https://doi.org/10.1016/j.phrs.2016.04.023>.
- Choi, Y., Kim, J.K., Lee, H.S., Hur, W.J., Hong, Y.S., Park, S., et al., 2006. Influence of intravenous contrast agent on dose calculations of intensity modulated radiation therapy plans for head and neck cancer. *Radiother. Oncol.* **81** (2), 158–162. <https://doi.org/10.1016/j.radonc.2006.09.010>.
- Erik, A.A., Kavaz, E., Ilkbahar, S., Kara, U., Erik, C., Tekin, H., 2019. Structural and photon attenuation properties of different types of fiber post materials for dental radiology applications. *Results. Phys.* **13**, 102354.
- Francis, Z., Incerti, S., Karamitros, M., Tran, H.N., Villagrasa, C., 2011. Nuclear Instruments and Methods in Physics Research B Stopping power and ranges of electrons, protons and alpha particles in liquid water using the Geant4-DNA package. *Nucl. Instrum. Methods Phys. Res. B* **269** (20), 2307–2311. <https://doi.org/10.1016/j.nimb.2011.02.031>. URL: <https://doi.org/10.1016/j.nimb.2011.02.031>.
- Gaikwad, D.K., Sayyed, M.I., Obaid, S.S., Issa, S.A.M., 2018. Pawar, P.P. Gamma ray shielding properties of TeO₂-ZnF₂-As₂O₃-Sm₂O₃ glasses. *J. Alloy. Comp.* **765**, 451–458. URL: <http://www.sciencedirect.com/science/article/pii/S0925838818323612>. <https://doi.org/10.1016/j.jallcom.2018.06.240>.
- Hine, G.J., 1952. The effective atomic numbers of materials for various gamma ray processes. *Phys. Rev.* **85**, 725.
- Hubbell, J.H., 1979. O/verbo/, I. Relativistic atomic form factors and photon coherent scattering cross sections. *J. Phys. Chem. Ref. Data* **8** (1), 69–106.
- Hubbell, J.H., 1999. Review of photon interaction cross section data in the medical and biological context. *Phys. Med. Biol.* **44** (1), 1–22. <https://doi.org/10.1088/0031-9155/44/1/001>.
- Hubbell, J., Veigele, W.J., Briggs, E., Brown, R., Cromer, D., Howerton, d.R., 1975. Atomic form factors, incoherent scattering functions, and photon scattering cross sections. *J. Phys. Chem. Ref. Data* **4** (3), 471–538.
- Issa, S.A., Saddeek, Y.B., Tekin, H.O., Sayyed, M.I., saber Shaaban, K., 2018. Investigations of radiation shielding using Monte Carlo method and elastic properties of PbO-SiO₂-B₂O₃-Na₂O glasses. *Curr. Appl. Phys.* **18** (6), 717–727. <https://doi.org/10.1016/j.cap.2018.02.018>. URL: <https://doi.org/10.1016/j.cap.2018.02.018>.
- Kilicoglu, O., Tekin, H.O., Singh, V.P., 2019. Determination of mass attenuation coefficients of different types of concretes using Monte Carlo method. *Eur. J. Sci. Technol.* **15**), 591–598.
- Kurudirek, M., 2014a. Effective atomic numbers and electron densities of some human tissues and dosimetric materials for mean energies of various radiation sources relevant to radiotherapy and medical applications. *Radiat. Phys. Chem.* **102**, 139–146. <https://doi.org/10.1016/j.radphyschem.2014.04.033>. URL: <https://doi.org/10.1016/j.radphyschem.2014.04.033>.
- Kurudirek, M., 2014b. Effective atomic numbers, water and tissue equivalence properties of human tissues, tissue equivalents and dosimetric materials for total electron interaction in the energy region 10keV-1GeV. *Appl. Radiat. Isot.* **94**, 1–7. <https://doi.org/10.1016/j.apradiso.2014.07.002>. URL: <https://doi.org/10.1016/j.apradiso.2014.07.002>.
- Kurudirek, M., 2017. Effective atomic number of soft tissue, water and air for interaction of various hadrons, leptons and isotopes of hydrogen. *Int. J. Radiat. Biol.* **93** (12), 1299–1305.
- Kurudirek, M., Chutithanapanon, N., Laopaiboon, R., Yenchai, C., Bootjomchai, C., 2018. Effect of Bi₂O₃ gamma ray shielding and structural properties of borosilicate glasses recycled from high pressure sodium lamp glass. *J. Alloy. Comp.* **745**, 355–364. <https://doi.org/10.1016/j.jallcom.2018.02.158>. URL: <https://doi.org/10.1016/j.jallcom.2018.02.158>.
- Lee, N., Choi, S.H., Hyeon, T., 2013. Nano-sized CT contrast agents. *Adv. Mater.* **25** (19), 2641–2660. <https://doi.org/10.1002/adma.201300081>.
- Lusic, H., Grinstaff, M.W., 2012. X-ray-computed tomography contrast agents. *Chem. Rev.* **113** (3), 1641–1666.
- Medhat, M., Singh, V., 2014. Mass attenuation coefficients of composite materials by geant4, xcom and experimental data: comparative study. *Radiat. Eff. Defects Solids* **169** (9), 800–807.
- Nowotny, R. Xmuat, 1998. Photon Attenuation Data on Pc. IAEA Report IAEA-NDS, pp. 195.
- Ramm, U., Damrau, M., Mose, S., Manegold, K.H., Rahl, C.G., Böttcher, H.D., 2001. Influence of CT contrast agents on dose calculations in a 3D treatment planning system. *Phys. Med. Biol.* **46** (10), 2631–2635. <https://doi.org/10.1088/0031-9155/46/10/308>.
- Sayyed, M.I., Qashou, S.I., Khattari, Z.Y., 2017. Radiation shielding competence of newly developed TeO₂-WO₃ glasses. *J. Alloy. Comp.* **696**, 632–638. <https://doi.org/10.1016/j.jallcom.2016.11.160>. URL: <https://doi.org/10.1016/j.jallcom.2016.11.160>.
- Sayyed, M., Ali, A., Tekin, H., Rammah, Y., 2019a. Investigation of gamma-ray shielding properties of bismuth borotellurite glasses using mcnp code and xcom program. *Appl. Phys. A* **125** (6), 445.
- Sayyed, M., El-Mesady, I., Abouhaswa, A., Askin, A., Rammah, Y., 2019b. Comprehensive study on the structural, optical, physical and gamma photon shielding features of b₂o₃-bi₂o₃-pbo-tio₂ glasses using winxcom and geant4 code. *J. Mol. Struct.* **1197**, 656–665.
- Sayyed, M.I., Lakshminarayana, G., Kaçal, M.R., Akman, F., 2019c. Radiation protective characteristics of some selected tungstates. *Radiochim. Acta* **107** (4), 349–357.
- Sharma, A., Sayyed, M., Agar, O., Tekin, H., 2019. Simulation of shielding parameters for teo₂-wo₃-geo₂ glasses using fluka code. *Results. Phys.* **13**, 102199.
- Shimizu, M., Kaneda, M., Hayakawa, T., Tsuchida, H., Itoh, A., 2009. Nuclear instruments and methods in physics research B stopping cross sections of liquid water for MeV energy protons. *Nucl. Instrum. Methods Phys. Res. B* **267** (16), 2667–2670. <https://doi.org/10.1016/j.nimb.2009.05.036>. URL: <https://doi.org/10.1016/j.nimb.2009.05.036>.
- Singh, V.P., Badiger, N.M., 2013. Study of effective atomic numbers and electron densities, kerma of alcohols, phantom and human organs, and tissues substitutes. *Nucl. Technol. Radiat. Prot.* **28** (2), 137–145. <https://doi.org/10.2298/NTRP1302137S>.
- Singh, V.P., Medhat, M.E., Badiger, N.M., 2014. Photon attenuation coefficients of thermoluminescent dosimetric materials by Geant4 toolkit, XCOM program and experimental data: a comparison study. *Ann. Nucl. Energy* **68**, 96–100. <https://doi.org/10.1016/j.anucene.2014.01.011>. URL: <https://doi.org/10.1016/j.anucene.2014.01.011>.
- Singh, V.P., Medhat, M.E., Badiger, N.M., 2015a. Photon energy absorption coefficients for nuclear track detectors using Geant4 Monte Carlo simulation. *Radiat. Phys. Chem.* **106**, 83–87. <https://doi.org/10.1016/j.radphyschem.2014.07.001>. URL: <https://doi.org/10.1016/j.radphyschem.2014.07.001>.
- Singh, V., Shirmardi, S., Medhat, M., Badiger, N., 2015b. Determination of mass attenuation coefficient for some polymers using Monte Carlo simulation. *Vacuum* **119**, 284–288. <https://doi.org/10.1016/j.vacuum.2015.06.006>. URL: <http://linkinghub.elsevier.com/retrieve/pii/S0042207X15002687>.
- Singh, V.P., Medhat, M.E., Shirmardi, S.P., 2015c. Comparative studies on shielding properties of some steel alloys using Geant4, MCNP, WinXCOM and experimental results. *Radiat. Phys. Chem.* **106**, 255–260. <https://doi.org/10.1016/j.radphyschem.2014.07.002>. URL: <https://doi.org/10.1016/j.radphyschem.2014.07.002>.
- Tekin, H., Altunsoy, E., Kavaz, E., Sayyed, M., Agar, O., Kamislioglu, M., 2019. Photon and neutron shielding performance of boron phosphate glasses for diagnostic radiology facilities. *Results. Phys.* **12**, 1457–1464.
- Thomsen, H.S., Stacul, F., Webb, J.A., 2014. Contrast medium-induced nephropathy. *In: Contrast Media*. Springer, pp. 81–104.
- Tonguc, B.T., Arslan, H., Al-Buriah, M.S., 2018. Studies on mass attenuation coefficients, effective atomic numbers and electron densities for some biomolecules. *Radiat. Phys. Chem.* **153**, 86–91. URL: <http://www.sciencedirect.com/science/article/pii/S0969806X18304778>. <https://doi.org/10.1016/j.radphyschem.2018.08.025>.
- Turhan, M.F., Durak, R., Akman, F., Kaçal, M.R., Araz, A., 2019. Determination of some selected absorption parameters for cd, la and ce elements. *Radiat. Phys. Chem.* **156**, 101–108.